

# Experimental Study on Composite Material Using Carbon Nanotubes

<sup>[1]</sup> Rishabh Singh, <sup>[2]</sup> Dr. Madan Chandra Maurya

<sup>[1]</sup><sup>[2]</sup> Madan Mohan Malaviya University of Technology, Gorakhpur, Uttar Pradesh, India  
Corresponding Author Email: <sup>[1]</sup> rishabh7997@gmail.com, <sup>[2]</sup> madanmaurya2001@gmail.com

---

**Abstract**— This research presents a detailed experimental investigation into the impact of carbon nanotube (CNT) reinforcement on the mechanical properties of composite materials. Carbon nanotubes, with their exceptional mechanical strength and unique structural characteristics, have gained prominence as potential reinforcing agents in composites. The study systematically explores the influence of varying concentrations of CNTs on the mechanical performance of the composite material. The experimental methodology involves the synthesis and characterization of composite specimens with different weight fractions of CNTs, employing a cutting-edge fabrication process. The mechanical properties are thoroughly assessed through a series of tests, including tensile tests to evaluate strength and elongation, flexural tests for bending strength and stiffness and hardness tests to gauge material resistance to indentation. Results from the mechanical tests reveal a significant enhancement in the strength, stiffness, toughness, and hardness of the composite material with the incorporation of CNTs. Tensile tests demonstrate improved load-bearing capabilities, while flexural tests highlight increased bending strength and stiffness. Impact tests reveal enhanced resistance to dynamic loading, and hardness tests showcase the reinforcement effect of CNTs on surface resistance. Microstructural analysis provides insights into the dispersion and alignment of CNTs within the matrix, elucidating the mechanisms responsible for the observed improvements in mechanical properties. The findings from this study contribute valuable knowledge for the development of advanced composite materials tailored for applications demanding superior mechanical performance. In conclusion, this experimental study sheds light on the synergistic effects of integrating carbon nanotubes into composite materials, specifically focusing on the enhancement of mechanical properties. The outcomes have implications for the design and engineering of advanced materials with improved strength, toughness, and hardness for a broad range of applications.

**Index Terms**— Composite material, Carbon Nanotubes, Tensile strength, Flexural strength, Hardness test.

---

## I. INTRODUCTION

This research project delves into a thorough experimental study on composite materials utilizing carbon nanotubes (CNTs) as reinforcing elements within an araldite resin matrix. Carbon nanotubes, renowned for their exceptional mechanical, electrical, and thermal properties, offer significant potential to enhance the overall performance of composite materials. The study systematically explores the effects of varied CNT concentrations on the mechanical properties of the composite material, with a specific focus on utilizing araldite resin as the matrix. The experimental methodology involves the synthesis and detailed characterization of composite specimens, integrating different weight fractions of CNTs and araldite resin through advanced fabrication techniques. Mechanical testing plays a pivotal role, encompassing flexural tests to assess bending strength, hardness tests to gauge resistance to indentation, and tensile tests to measure strength and elongation. Through a comprehensive suite of mechanical tests, this study aims to unveil the impact of CNTs and araldite resin on the composite material's mechanical behavior. The research seeks to provide insights into the combined effects of these constituents on flexural strength, hardness, and tensile properties, contributing to a holistic understanding of the synergies between carbon nanotubes and araldite resin matrices. Microstructural analysis forms an integral part of the study, offering valuable information on the dispersion and

alignment of CNTs within the araldite resin matrix. This analysis aims to unravel the underlying mechanisms responsible for observed changes in material properties, providing a comprehensive view of the nanotube-matrix interaction within the context of araldite resin. The findings of this experimental study hold significant implications for the development of advanced composite materials with improved mechanical characteristics. This research contributes valuable insights to offer a lightweight and flexible solution for retrofitting structures, providing adaptive reinforcements that conform to damaged areas, particularly corners and edges. Additionally, the cost-effectiveness of these composite materials, combined with their ease of installation, presents a practical solution for seismic retrofitting, potentially reducing labour and overall retrofitting costs. Overall, the necessity for these composite materials arises from the imperative to fortify structures against seismic forces efficiently, economically, and in an environmentally sustainable manner.

## II. MATERIAL AND METHODOLOGY

### A. Material:

The composite material sheet is a synergistic blend of specific constituents, each chosen for its unique properties. The primary materials include araldite resin as the matrix, jute mesh as an eco-friendly reinforcing material, and carbon nanotubes (CNTs) of various types for advanced mechanical

strength. Specifically Single-Walled Carbon Nanotubes (SWCNTs), Multi-Walled Carbon Nanotubes (MWCNTs), Araldite LY-556, Hardener HY-951, Jute Mesh, Acetone.

### B. Methodology:

The methodology for preparing composite sheets using Araldite epoxy resin, jute mesh, and carbon nanotubes via hand-lay method involves several key steps. Firstly, the materials are meticulously measured and prepared, ensuring a clean workspace and appropriate personal protective equipment. Next, the Araldite epoxy resin is mixed with carbon nanotubes using acetone and stirred with magnetic stirrer until a homogeneous mixture is achieved. The hand-lay process begins by layering the composite mixture onto a flat surface, then placing a sheet of jute mesh and again place a layer of epoxy CNT mix, repeating the process to create multiple uniform layers. Pressure is applied to remove air bubbles, and the composite is left for 24 hrs under dead load. After 24hrs standardized samples are prepared from the composite sheets for mechanical testing, including tensile strength, flexural strength, and hardness. Concurrently, virtual models of the composite samples are created using Abaqus software, with corresponding material properties and boundary conditions applied. Simulations are conducted to analyse mechanical behaviour under various loading conditions. Subsequent comparison between physical test results and Abaqus simulations allows for evaluation of the simulation model's accuracy. Any disparities are analysed to identify contributing factors, potentially leading to optimization of composite formulation or simulation parameters. Finally, comprehensive documentation and reporting of the methodology, results, and conclusions are compiled for further analysis and reference.

### C. Physical Sample Fabrication Steps:

(a) *Sonication of CNTs in acetone solvent:* In this procedure, 100g of acetone is placed in a conical flask, followed by the addition of the required amount of CNTs. The mixture is then stirred using a magnetic stirrer at 500 RPM for 30 minutes. Fig 2(A). Subsequently, the mixture is transferred to an ultrasonic cleaner and subjected to treatment for another 30 minutes.

(b) *Fusion of CNTs in araldite:* On the other hand, we need to heat the epoxy resin to 120 degrees Celsius and continuously stir it at 500 RPM for about 30 minutes (see Fig 2(B)). Once both mixes are prepared, pour the CNT mix into the hot epoxy and continue stirring at 500 RPM for another 30 minutes (Fig 2(C)). Then, place the mixture in an ultrasonic cleaner for an additional 30 minutes (Fig 2(D)).

(c) *Preparation of sample plate:* We are utilizing the hand-lay technique to produce a composite fiber sheet. Initially, the composite solution is spread onto a metal sheet to create the first layer (Fig 3(A)). Then, a layer of jute mesh is placed on top (Fig 3(B)) then spread another layer of composite solution over jute sheet (Fig 3(C)) and compressed

to ensure complete saturation with the epoxy mixture. This process is repeated four times, with each layer of jute mesh being fully infused with epoxy solution. See Figure 2(D) for visual reference.

(d) *Application of dead load:* During this procedure, the lead load is applied to the metal plate to eliminate any air voids, ensuring proper compression of the sheet. The load is left in place for approximately 24 hours to allow for settling.

(e) *Demolding:* After 24 hours, the sheet was removed from the metal mold, and now the sheets are prepared for testing.

### D. Hand-lay method:

The hand layup method is a manual process used in manufacturing composite materials. It involves applying layers of resin and reinforcement materials, such as fibers or fabric, by hand onto a mold or substrate. This method allows for flexibility in design and is commonly used for producing prototypes or small-scale production runs. However, it can be labor-intensive and may result in variations in quality compared to automated processes.



**Fig 1: Hand-lay Method**

## III. SAMPLE PREPARATION

The sample is prepared as per the ASTM standards. The following are the ASTM standards are used to perform the sample testing.

**Table 1: ASTM Standards**

S. No.	ASTM Standards	Description
1.	ASTM D3039	Code for Tensile Properties of Polymer Matrix Composite Materials.
2.	ASTM D7264	Code for Flexural Properties of Polymer Matrix Composite Materials.
3.	ASTM D785	Code of Determining Rockwell Hardness of Plastics and Electrical Insulating Materials.

### A. Sample Sizing.

Flexure Sample Size = 250 X 25 X 2.5

Tensile Sample Size = 100 X 15 X 2.5

Hardness Testing Sample = 30 X 30 X 2.5

**Table 2:** No. of Samples for each test.

S. No	Test Name	Sample Type	No. of sample
1.	Tensile Testing	Single walled CNT 0.1%	3
2.		Single walled CNT 0.3%	3
3.		Single walled CNT 0.5%	3
4.		Multi walled CNT 0.1%	3
5.		Multi walled CNT 0.3%	3
6.		Multi walled CNT 0.5%	3
7.	Flexure Testing	Single walled CNT 0.1%	3
8.		Single walled CNT 0.3%	3
9.		Single walled CNT 0.5%	3
10.		Multi walled CNT 0.1%	3
11.		Multi walled CNT 0.3%	3
12.		Multi walled CNT 0.5%	3
13.	Hardness Testing	Single walled CNT 0.1%	3
14.		Single walled CNT 0.3%	3
15.		Single walled CNT 0.5%	3
16.		Multi walled CNT 0.1%	3
17.		Multi walled CNT 0.3%	3
18.		Multi walled CNT 0.5%	3

Total No. of Samples = **54 samples.** (Fig 4)

**IV. PHYSICAL TEST OVERVIEW**

**A. Tensile Testing:**

Tensile testing measures a material's strength by subjecting it to controlled tension until it breaks. An intrusion machine, equipped with grips, gradually stretches the material while recording its response. This method assesses properties like ultimate tensile strength and yield strength, which is quite essential in engineering and material science for determining the maximum stress a material can withstand without breaking when subjected to stretching or pulling force.

**B. Flexure Testing:**

Flexure testing evaluates a material's resistance to bending or flexing forces. A specimen is placed on supports and subjected to a load at its midpoint, causing it to bend until failure. This test measures properties like modulus of elasticity and flexural strength, crucial for assessing material suitability in structural applications.

**C. Durometer Hardness Testing:**

Hardness testing via a Durometer hardness testing machine assesses a material's resistance to indentation. In our test the specimen is a composite hence the indenter used is the Shore D scale indenter is used as the thickness of the material is very less and the material is hard. The indenter is pressed into the material under a specific load, and the depth of

penetration is measured. This method provides valuable data for material selection and quality control in manufacturing and metallurgy

**V. RESULT**

**A. Flexure Test Report:**

Specimen Specification

Gage Length: 80

Rate: 2mm/min

Facility: MTL, ACMS IIT Kanpur

Instrument: INSTRON\_1195 (retrofitted by BiSS, India)

Test Type: Flexural



**Fig 2:** Flexure Testing Machine

**Highest Flexural Peak Stress from Each Sample Set.**

**(a) Specimen Code: MFA3**

Flexural Peak Stress = 84.786MPa

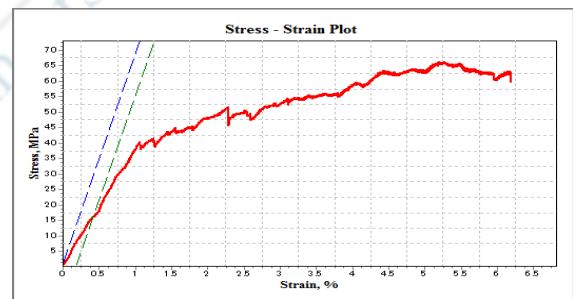


**Fig 3:** Experimental Flexural Stress-Strain Curve

**(b) Specimen Code: MFB1**

Flexural Peak Stress = 80.32MPa

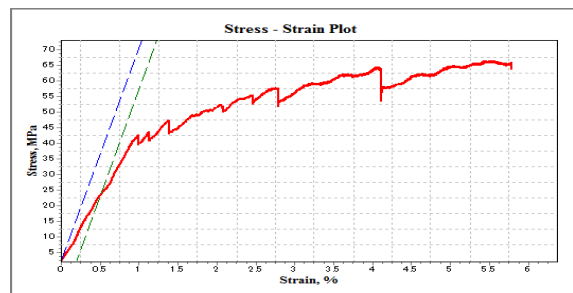


**Fig 4:** Experimental Flexural Stress-Strain Curve



**(c) Specimen Code: MFC1**

Flexural Peak Stress = 102.36MPa

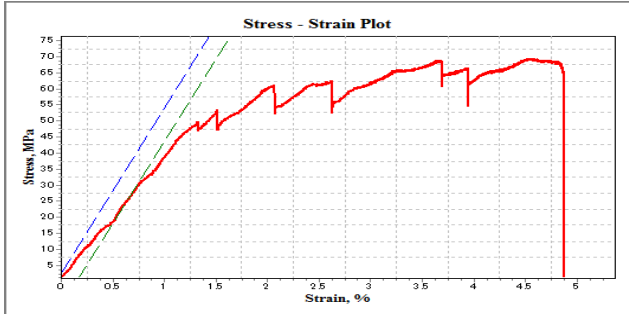


**Fig 5:** Experimental Flexural Stress-Strain Curve

**(e) Specimen Code: SFB3**

Flexural Peak Stress = 89.405MPa



**Fig 7:** Experimental Flexural Stress-Strain Curve

**(d) Specimen Code: SFA3**

Flexural Peak Stress = 75.05MPa

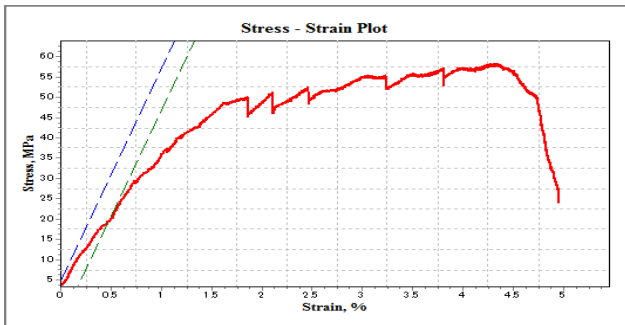


**Fig6:** Experimental Flexural Stress-Strain Curve

**(f) Specimen Code: SFC2**

Flexural Peak Stress = 68.999MPa

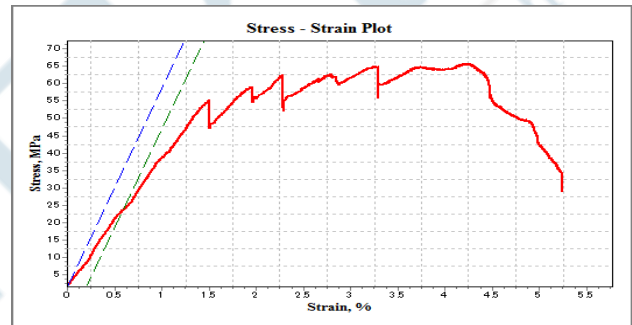


**Fig 8:** Experimental Flexural Stress-Strain Curve

**Table 3:** Summary of experimental flexure testing:

S. No	Specimen ID	Gauge Length	Loading Rate (mm/min)	Span (mm)	Width (mm)	Thickness (mm)	Flexural Peak Stress (MPa)	Offset Flexural Yield Stress (MPa)	Offset Flexural Yield Load (KN)	Displacement (mm)
1	MFA1	80	2	80	14.99	2.36	<b>65.039</b>	0.01	0.01	<b>17</b>
2	MFA2	80	2	80	15.15	2.57	<b>69.628</b>	0.013	0.013	<b>16</b>
3	MFA3	80	2	80	15.38	2.2	<b>84.786</b>	0.01	0.01	<b>11</b>
	AVG	80	2	80	15.173333	2.37666667	<b>73.151</b>	0.011	0.011	<b>14.7</b>
4	MFB1	80	2	80	15.03	2.47	<b>80.32</b>	0.014	0.014	<b>12</b>
5	MFB2	80	2	80	15.01	2.48	<b>76.958</b>	0.013	0.013	<b>11</b>
6	MFB3	80	2	80	15.13	2.5	<b>64.178</b>	0.011	0.011	<b>15</b>
	AVG	80	2	80	15.056667	2.48333333	<b>73.81866667</b>	0.012666667	0.012666667	<b>12.7</b>
7	MFC1	80	2	80	14.83	2.25	<b>102.36</b>	0.012	0.012	<b>9</b>
8	MFC2	80	2	80	15.05	2.73	<b>81.115</b>	0.015	0.015	<b>10</b>
9	MFC3	80	2	80	15.1	2.32	<b>93.436</b>	0.012	0.012	<b>12</b>
	AVG	80	2	80	14.993333	2.43333333	<b>92.30366667</b>	0.013	0.013	<b>10.4</b>
10	SFA1	80	2	80	15.05	2.35	<b>65.049</b>	0.013	0.013	<b>16</b>
11	SFA2	80	2	80	15	2.37	<b>67.927</b>	0.014	0.014	<b>12</b>
12	SFA3	80	2	80	15	2.45	<b>75.05</b>	0.013	0.013	<b>8</b>
	AVG	80	2	80	15.016667	2.39	<b>69.342</b>	0.013333333	0.013333333	<b>12</b>
13	SFB1	80	2	80	15.57	2.71	<b>67.891</b>	0.019	0.019	<b>11</b>

S. No	Specimen ID	Gauge Length	Loading Rate (mm/min)	Span (mm)	Width (mm)	Thickness (mm)	Flexural Peak Stress (MPa)	Offset Flexural Yield Stress (MPa)	Offset Flexural Yield Load (KN)	Displacement (mm)
14	SFB2	80	2	80	15.56	2.47	<b>62.331</b>	0.015	0.015	<b>14</b>
15	SFB3	80	2	80	15.23	2.9	<b>89.405</b>	0.022	0.022	<b>8</b>
	AVG	80	2	80	15.453333	2.693333333	<b>73.209</b>	0.018666667	0.018666667	<b>11</b>
16	SFC1	80	2	80	15.14	2.38	<b>66.64</b>	0.014	0.014	<b>12</b>
17	SFC2	80	2	80	15	2.48	<b>68.999</b>	0.016	0.016	<b>10</b>
18	SFC3	80	2	80	15	2.36	<b>67.861</b>	0.014	0.014	<b>12</b>
	AVG	80	2	80	15.046667	2.406666667	<b>67.83333333</b>	0.014666667	0.014666667	<b>11.4</b>

**Table 4:** Summary of software flexure testing

S. No	Specimen ID	Gauge Length (mm)	Span (mm)	Width (mm)	Depth (mm)	Flexural Peak Stress [Software] (MPa)
1	MFA1	80	100	15	2.5	<b>72.70</b>
2	MFA2	80	100	15	2.5	<b>83.90</b>
3	MFA3	80	100	15	2.5	<b>83.97</b>
	AVG	80	100	15	2.5	<b>80.19</b>
4	MFB1	80	100	15	2.5	<b>84.48</b>
5	MFB2	80	100	15	2.5	<b>80.21</b>
6	MFB3	80	100	15	2.5	<b>72.80</b>
	AVG	80	100	15	2.5	<b>79.16</b>
7	MFC1	80	100	15	2.5	<b>95.12</b>
8	MFC2	80	100	15	2.5	<b>89.01</b>
9	MFC3	80	100	15	2.5	<b>99.00</b>
	AVG	80	100	15	2.5	<b>94.37</b>
10	SFA1	80	100	15	2.5	<b>64.22</b>
11	SFA2	80	100	15	2.5	<b>72.21</b>
12	SFA3	80	100	15	2.5	<b>81.26</b>
	AVG	80	100	15	2.5	<b>72.56</b>
13	SFB1	80	100	15	2.5	<b>65.21</b>
14	SFB2	80	100	15	2.5	<b>67.95</b>
15	SFB3	80	100	15	2.5	<b>92.15</b>
	AVG	80	100	15	2.5	<b>75.11</b>
16	SFC1	80	100	15	2.5	<b>71.00</b>
17	SFC2	80	100	15	2.5	<b>75.50</b>
18	SFC3	80	100	15	2.5	<b>72.25</b>
	AVG	80	100	15	2.5	<b>72.92</b>

**Table 5:** Comp. b/w exp. and soft. flexure testing

S. No	Specimen ID	Flexural Peak Stress (MPa) [EXPERIMENTAL]	Flexural Peak Stress (MPa) [SOFTWARE]
1	MFA1	<b>65.039</b>	<b>72.7</b>
2	MFA2	<b>69.628</b>	<b>83.90</b>
3	MFA3	<b>84.786</b>	<b>83.97</b>
	AVG	<b>73.151</b>	<b>80.19</b>
4	MFB1	<b>80.32</b>	<b>79</b>
5	MFB2	<b>76.958</b>	<b>91.2</b>
6	MFB3	<b>64.178</b>	<b>72.8</b>
	AVG	<b>73.81866667</b>	<b>82</b>
7	MFC1	<b>102.36</b>	<b>82.3</b>
8	MFC2	<b>81.115</b>	<b>98</b>
9	MFC3	<b>93.436</b>	<b>94.01</b>
	AVG	<b>92.30366667</b>	<b>91.43</b>
10	SFA1	<b>65.049</b>	<b>42.4</b>
11	SFA2	<b>67.927</b>	<b>89.7</b>
12	SFA3	<b>75.05</b>	<b>97.4</b>
	AVG	<b>69.342</b>	<b>76.36</b>
13	SFB1	<b>67.891</b>	<b>83.9</b>
14	SFB2	<b>62.331</b>	<b>76.1</b>
15	SFB3	<b>89.405</b>	<b>71.7</b>
	AVG	<b>73.209</b>	<b>77.033</b>
16	SFC1	<b>66.64</b>	<b>88.29</b>
17	SFC2	<b>68.999</b>	<b>53.59</b>
18	SFC3	<b>67.861</b>	<b>89.17</b>
	AVG	<b>67.83</b>	<b>77.016</b>

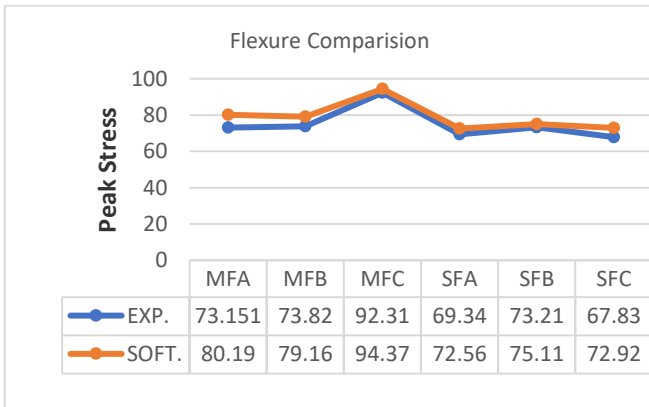


**Fig 9:** Comparison between experimental and software flexure testing

**B. Experimental Tensile Testing Report**

Area: 62.95 sq-mm  
 Gage Length: 50.11 mm  
 Rate: 1 mm/min  
 Facility: MTL, ACMS IIT Kanpur  
 Instrument: BiSS 100kN UTM (Hydraulic)  
 Test Mode: Tensile

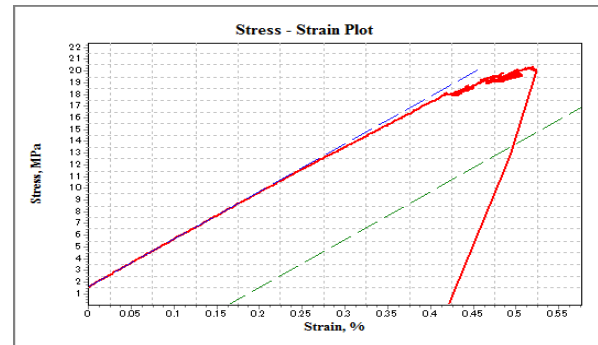


**Fig 10** Tensile Testing Machine

*Highest Tensile Peak Stress from Each Sample Set.*

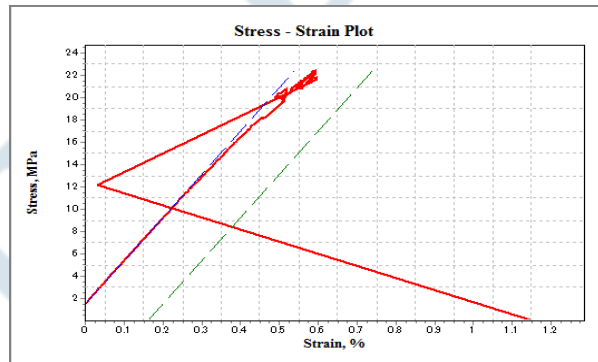
**(a) Specimen Code: MTA1**

Tensile Peak Stress = 20.333MPa



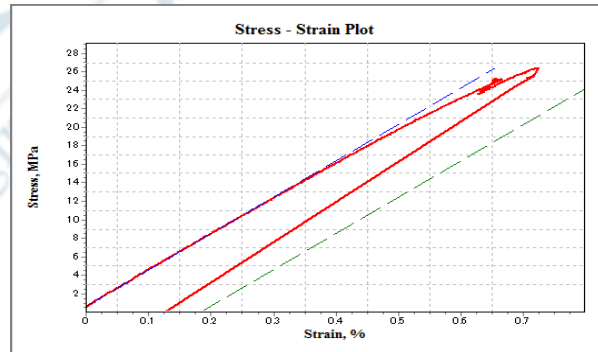
**Fig 11:** Experimental Tensile Stress-Strain Curve  
**(b) Specimen Code: MTB3**

Tensile Peak Stress = 22.443MPa



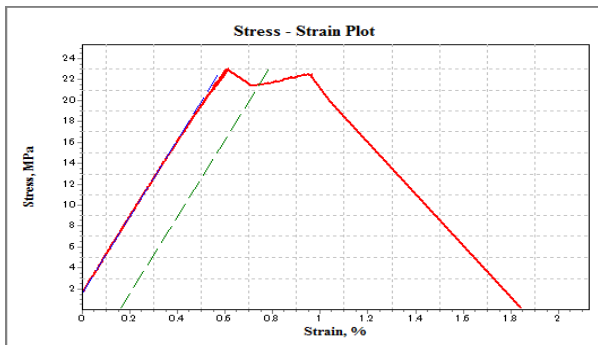
**Fig 12:** Experimental Tensile Stress-Strain Curve  
**(c) Specimen Code: MTC3**

Tensile Peak Stress = 26.441MPa



**Fig 13:** Experimental Tensile Stress-Strain Curve  
**(d) Specimen Code: STA1**

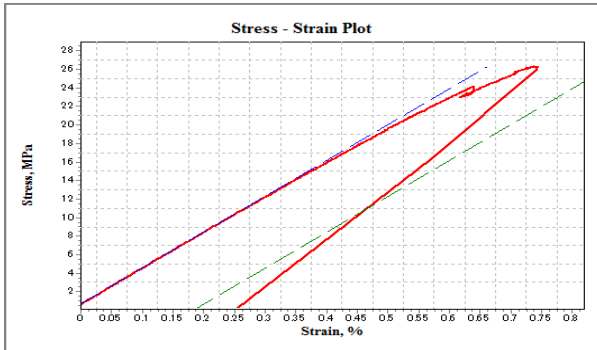
Tensile Peak Stress = 23.038MPa



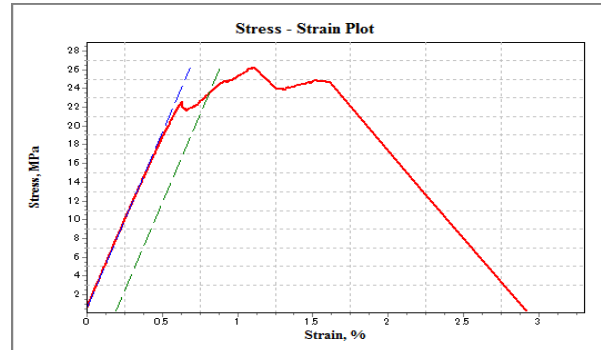
**Fig 14:** Experimental Tensile Stress-Strain Curve

**(e) Specimen Code: STB3**

Tensile Peak Stress = 26.283MPa


**Fig 15: Experimental Tensile Stress-Strain Curve**
**(f) Specimen Code: STC3**

Tensile Peak Stress = 26.335MPa


**Fig 16: Experimental Tensile Stress-Strain Curve**
**Table 6: Summary of experimental tensile testing**

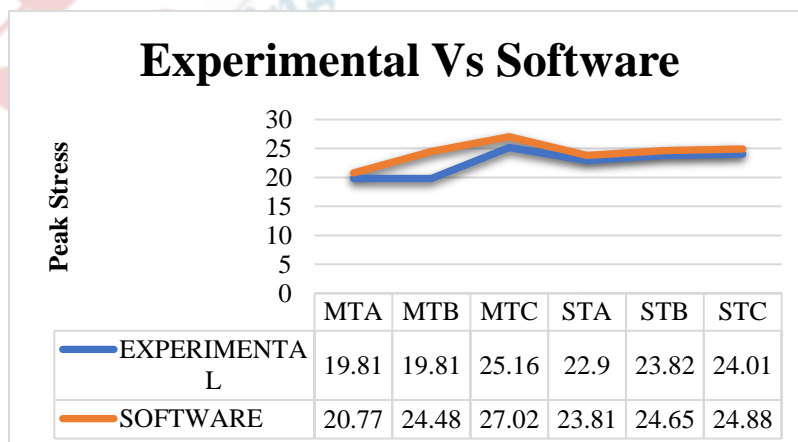
S. No	Specimen ID	Gauge Length	Loading Rate (mm/min)	Width (mm)	Thickness (mm)	Tensile Peak Stress (MPa)	0.2% Offset Yield Stress (MPa)	Yield Strain %	Modulus	Elongation at Break (Using Strain)
1	MTA1	50	1	25.18	2.5	20.333	12.78	0.493	4.071	0.414
2	MTA2	50	1	25.17	2.6	19.224	17.697	0.636	3.644	4.245
3	MTA3	50	1	25	2.56	19.877	18.599	0.67	3.626	3.445
	<b>AVG</b>	<b>50</b>	<b>1</b>	<b>25.116</b>	<b>2.453</b>	<b>19.810</b>	<b>16.358</b>	<b>0.599</b>	<b>3.7803</b>	<b>2.701</b>
4	MTB1	50	1	25.22	2.4	23.403	0	0	4.038	0.602
5	MTB2	50	1	25.85	2.4	23.074	13.773	0.578	3.701	0.533
6	MTB3	50	1	25.1	2.5	22.443	0	0	3.877	1.169
	<b>AVG</b>	<b>50</b>	<b>1</b>	<b>25.39</b>	<b>2.433</b>	<b>22.97</b>	<b>4.591</b>	<b>0.1926</b>	<b>3.872</b>	<b>0.768</b>
7	MTC1	50	1	25.18	2.58	22.671	0	0	3.35	0.316
8	MTC2	50	1	25.1	2.52	26.37	23.719	0.765	3.912	2.209
9	MTC3	50	1	25.09	2.2	26.441	0	0	3.932	0.143
	<b>AVG</b>	<b>50</b>	<b>1</b>	<b>25.123</b>	<b>2.433</b>	<b>25.160</b>	<b>7.906</b>	<b>0.255</b>	<b>3.731</b>	<b>2.572</b>
10	STA1	50	1	25.04	2.52	23.038	21.506	0.743	3.681	1.936
11	STA2	50	1	25.1	2.62	22.857	0	0	3.552	0.118
12	STA3	50	1	25.1	2.6	22.806	20.753	0.756	3.603	0.421
	<b>AVG</b>	<b>50</b>	<b>1</b>	<b>25.08</b>	<b>2.58</b>	<b>22.900</b>	<b>14.086</b>	<b>0.499</b>	<b>3.612</b>	<b>0.825</b>
13	STB1	50	1	25	2.7	21.406	19.816	0.731	3.487	1.9
14	STB2	50	1	25	2.68	23.771	20.604	0.745	3.533	1.691
15	STB3	50	1	25	2.3	26.283	23.465	0.811	3.74	3.005
	<b>AVG</b>	<b>50</b>	<b>1</b>	<b>25</b>	<b>2.56</b>	<b>23.82</b>	<b>21.295</b>	<b>0.762</b>	<b>3.586</b>	<b>2.1986</b>
16	STC1	50	1	25.18	2.58	22.619	16.874	0.657	3.723	0.817
17	STC2	50	1	25.1	2.52	23.059	10.563	0.67	3.812	0.742
18	STC3	50	1	25.1	2.4	26.335	0	0	3.878	0.238
	<b>AVG</b>	<b>50</b>	<b>1</b>	<b>25.126</b>	<b>2.5</b>	<b>24.004</b>	<b>9.145</b>	<b>0.442</b>	<b>3.804</b>	<b>0.599</b>

**Table 7:** Summary of software tensile testing

S. No	Specimen ID	Tensile Peak Stress (MPa) EXPERIMENTAL	Tensile Peak Stress (MPa) SOFTWARE
1	MTA1	20.333	21.3
2	MTA2	19.224	20.24
3	MTA3	19.877	20.78
	AVG	19.810	20.77
4	MTB1	23.403	24.88
5	MTB2	23.074	24.78
6	MTB3	22.443	23.78
	AVG	22.97	24.48
7	MTC1	22.671	24.86
8	MTC2	26.37	27.43
9	MTC3	26.441	28.77
	AVG	25.160	27.02
10	STA1	23.038	24.41
11	STA2	22.857	23.25
12	STA3	22.806	23.78
	AVG	22.900	23.81
13	STB1	21.406	21.55
14	STB2	23.771	21.77
15	STB3	26.283	28.45
	AVG	23.82	23.92
16	STC1	22.619	28.28
17	STC2	23.059	23.47
18	STC3	26.335	26.44
	AVG	24.004	26.06

**Table 8:** Comp. b/w exp. and soft. tensile testing.

S. No	Specimen ID	Gauge Length (mm)	Width (mm)	Thickness (mm)	Tensile Peak Stress (MPa)
1	MTA1	50	25	2.5	21.3
2	MTA2	50	25	2.5	20.24
3	MTA3	50	25	2.5	20.78
	AVG	50	25	2.5	20.77
4	MTB1	50	25	2.5	24.88
5	MTB2	50	25	2.5	24.78
6	MTB3	50	25	2.5	23.78
	AVG	50	25	2.5	24.48
7	MTC1	50	25	2.5	24.86
8	MTC2	50	25	2.5	27.43
9	MTC3	50	25	2.5	28.77
	AVG	50	25	2.5	27.02
10	STA1	50	25	2.5	24.41
11	STA2	50	25	2.5	23.25
12	STA3	50	25	2.5	23.78
	AVG	50	25	2.5	23.81
13	STB1	50	25	2.5	21.55
14	STB2	50	25	2.5	23.74
15	STB3	50	25	2.5	28.45
	AVG	50	25	2.5	24.58
16	STC1	50	25	2.5	24.74
17	STC2	50	25	2.5	23.47
18	STC3	50	25	2.5	26.44
	AVG	50	25	2.5	28.88


**Fig 17:** Comp. b/w exp. and soft, tensile testing



**C. Hardness Test**

Sample Specification  
Dimension: 30 X 30 mm  
Thickness: 2.5mm  
Indenter Type: D-Shore

S. No	Specimen ID	Shore (D) Hardness Test
1	MHA1	76
2	MHA2	75
3	MHA3	79
	AVG	76.6
4	MHB1	81
5	MHB2	79
6	MHB3	80
	AVG	80
7	MHC1	83
8	MHC2	85
9	MHC3	80
	AVG	82.7
10	SHA1	78
11	SHA2	81
12	SHA3	80
	AVG	79.6
13	SHB1	81
14	SHB2	83
15	SHB3	79
	AVG	81
16	SHC1	79
17	SHC2	80
18	SHC3	83
	AVG	80.6



**Fig 18: Hardness Testing Machine**

**D. Fractography Test**

Scanning electron microscopy (SEM) is a valuable tool for examining failure modes in composite materials. Figures 19 illustrate various types of failures common in these materials, such as fiber breakage, fiber pull-out, and matrix cracking. Typically, matrix cracking is the initial failure mode, followed by fiber pull-out, and eventually fiber fracture. These failure mechanisms are typical in brittle composites, often due to poor adhesion between fibers and the matrix.

In terms of composite fracture mechanics, stress is initially borne by both the fibers and the matrix. As the matrix begins to crack, fibers can act as crack stoppers, delaying catastrophic failure until the matrix is significantly compromised. When tension increases, the primary cell wall can collapse, leading to fiber breakdown and loss of cell cohesion. Matrix cracks are indicative of brittle failure, which is a primary failure mechanism. Additionally, the presence of voids in the figures is related to fiber pull-out, with the distance between the fiber and the matrix indicating the strength of the fiber-matrix adhesion. These findings align with existing literature on composite failure patterns.

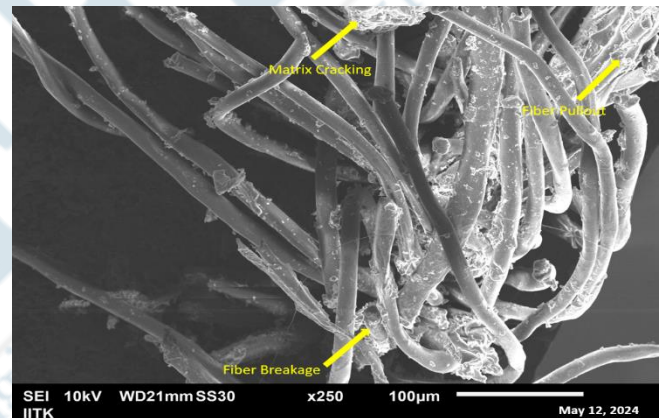


**Fig 19: Matrix Breaking, Fiber Breaking & Pullout**

**VI. CONCLUSIONS**

The current study examines the benefits of using the Carbon Nanotubes in the composite as a matrix in the preparation of composite sheet for different engineering works, especially for structural work. The effect of stacking sequences with different types of Carbon Nanotubes to the composite was investigated through physical sample and through the software. In this study, it can be proved that the mechanical properties of the composite can be improved by changing the stacking sequences of the lamination.

The study had drawn the following conclusion:

- The carbon nanotubes are treated with acetone to provide better binding with the araldite.
- The tensile strength of the composite with the 0.5% of MWCNT provide highest peak strength.
- The tensile strength of the composite having 0.5% of SWCNT is less effective the MWCNT with the same

configuration.

- The flexural strength of the composite with the 0.5% of MWCNT provide highest peak strength.
- The flexural strength of the composite having 0.5% of SWCNT is less effective the MWCNT with the same configuration.
- After comparing with the other composites having different fluxes and reinforcement the composites with CNTs are better alternatives.
- The composite made from CNTs have less thickness then the traditional composites.
- The highest flexural peak stress found in sample MFC3 which is 93.436MPa.
- The highest tensile peak stress found in sample MTC3 which is 26.441MPa.
- The maximum displacement found in sample MFA1 which is 17mm.
- Comparing the experimental and the analytical results, it was observed the there is a very slight variation in both the results.
- The composite can be used as a in retrofitting of the buildings.
- It can be used to retrofit the old structures without changing its aesthetic values.
- The composite developed can also be integrated with AI.
- SEM analysis gives the better view of the Fiber breakage, Fiber pulling and Matrix cracking.

## REFERENCES

- [1] Abdul Khalil, H. P.S., I. U.H. Bhat, M. Jawaid, A. Zaidon, D. Hermawan, and Y. S. Hadi. 2012. "Bamboo Fibre Reinforced Biocomposites: A Review." *Materials and Design* 42: 353–68. <https://doi.org/10.1016/j.matdes.2012.06.015>
- [2] Adeniyi, Adewale George, Samson Akorede Adeoye, Damilola Victoria Onifade, and Joshua O. Ighalo. 2021. "Multi-Scale Finite Element Analysis of Effective Elastic Property of Sisal Fiber-Reinforced Polystyrene Composites." *Mechanics of Advanced Materials and Structures* 28 (12):1245–53. <https://doi.org/10.1080/15376494.2019.1660016>
- [3] Alhijazi, Mohamad, Qasim Zeeshan, Zhaoye Qin, Babak Safaei, and Mohammed Asmael. 2020. "Finite Element Analysis of Natural Fibers Composites: A Review." *Nanotechnology Reviews* 9 (1): 853–75. <https://doi.org/10.1515/ntrev-2020-0069>
- [4] Doan, Thi Thu Loan, Hanna Brodowsky, and Edith Mäder. 2012. "Jute Fibre/Epoxy Composites: Surface Properties and Interfacial Adhesion." *Composites Science and Technology* 72 (10): 1160–66. <https://doi.org/10.1016/j.compscitech.2012.03.025>
- [5] Ramkumar, R., & Saravanan, P., 2020. Assessment of Composites using Waste Sugarcane Bagasse Fiber and Wood Dust Powder. *International Journal of Innovative Technology and Exploring Engineering*, 9(5), pp. 2126–2131. <https://doi.org/10.35940/ijtee.e3016.039520>
- [6] A. G., Onifade, D. V., Ighalo, J. O., & Adeoye, A. S., 2019. A review of coir fiber reinforced polymer composites. *Composites Part B: Engineering*, 176(June), 107305. <https://doi.org/10.1016/j.compositesb.2019.107305>
- [7] Mahesh, V., Joladarashi, S., & Kulkarni, S. M., 2019. An experimental study on adhesion, flexibility, interlaminar shear strength, and damage mechanism of jute/rubber-based flexible "green" composite. *Journal of Thermoplastic Composite Materials*, 35(2), pp. 1–28. <https://doi.org/https://doi.org/10.1177/0892705719882074>
- [8] Ramesh, M., 2016. Kenaf (*Hibiscus cannabinus* L.) fiber based on bio-materials: A review on processing and properties. *Progress in Materials Science*, 78–79, pp. 1–92. <https://doi.org/https://doi.org/10.1016/j.pmatsci.2015.11.001>
- [9] Rafiquzzaman, M., Taimum Islam, M., Raihan Hossain, M., Fazla Rabby, M., & Rifat Hashar, M., 2017. Fabrication and Performance Test of Glass-Bamboo Fiber Based Industry Safety Helmet. *American Journal of Mechanical and Materials Engineering*, 1(1), pp. 20–25. <https://doi.org/10.11648/j.ajmme.20170102.13>
- [10] Yahaya, R., Sapuan, S. M., Leman, Z., & Zainudin, E. S., 2014. Selection of natural fiber for hybrid laminated composites vehicle spall liners using analytical hierarchy process (AHP). *Applied Mechanics and Materials*, 564, pp. 400–405. <https://doi.org/10.4028/www.scientific.net/AMM.564.400>
- [11] Mohammed, I., Talib, A. R. A., Hameed Sultan, M. T., Jawaid, M., Ariffin, A. H., & Saadon, S., 2018. Mechanical properties of Fiber-metal laminates made of natural/synthetic fiber composites. *BioResources*, 13(1), pp. 2022–2034. <https://doi.org/10.15376/biores.13.1.2022-2034>
- [12] Feng, N. L., DharMalingam, S., Zakaria, K. A., & Selamat, M. Z., 2017. Investigation on the fatigue life characteristic of kenaf/glass woven-ply reinforced metal sandwich materials. *Journal of Sandwich Structures & Materials*, 21(7), pp. 2440–2455. <https://doi.org/10.1177/1099636217729910>
- [13] Rashdi, A. A. A., Sapuan, S. M., Ahmad, M. M. H. M., & Abdan, K. B., 2009. Review of kenaf fiber reinforced polymer composites. *Polimery/Polymers*, 54(11–12), pp. 777–780. <https://doi.org/10.14314/polimery.2009.777>
- [14] Yahaya, R., Sapuan, S., Jawaid, M., Leman, Z., & Zainudin, E., 2018. Review of Kenaf Reinforced Hybrid Biocomposites: Potential for Defence Applications. *Current Analytical Chemistry*, 14(3), pp. 226–240.
- [15] Chandrika, S., Kumar, T. R. H., & Mahesh, V., 2022. Physio-mechanical characterization of kenaf/saw dust reinforced polymer matrix composite and selection of optimal configuration using MADM-VIKOR approach. *International Journal on Interactive Design and Manufacturing*. <https://doi.org/10.1007/s12008-022-01078-7>
- [16] Mahesh, V., 2022. Development and Physio-Mechanical Characterization of Sustainable Jute-Wood Dust Reinforced Hybrid Composites. *Journal of Natural Fibers*, 19(16), pp. 13995–14004. <https://doi.org/10.1080/15440478.2022.2113852>
- [17] Prabu, V. A., Johnson, R. D. J., Amuthakkannan, P., & Manikandan, V., 2017. Usage of industrial wastes as particulate composite for environment management: Hardness, Tensile and Impact studies. *Journal of Environmental Chemical Engineering*, 5(1), pp. 1289–1301. <https://doi.org/https://doi.org/10.1016/j.jece.2017.02.007>